

Finite Element Analysis of Reinforced Concrete Sub-assembly under High Rate Loading in a Column Removal Scenario

Nima Usefi*, Reza Abbasnia and Foad Mohajeri Nav

Department of Civil Engineering, Iran University of Science and Technology, Tehran, Iran

*Corresponding author's Email: N_yusefi@civileng.iust.ac.ir

ABSTRACT: Progressive collapse is a dynamic event with high strain rate in which the failure of a member causes damage to the overall structure. Most research done in the field of progressive collapse are carried out with static analysis. Structural behaviour with regard to the effects of strain rate needs further studies. In this research, to investigate the effects of strain rate in a progressive failure, existing theories are used for Finite Element (FE) modelling of two sub-assemblages, previously tested under static loading. Confirming the model in the static mode, by increasing the rate of loading, the specimens are subjected to high strain rate condition in order to simulate the target scenario of progressive collapse. Results shows that considering the strain rate effects in the FE analysis, the strength of sub-assemblages in the compression zone increases, and the ultimate strength capacity decreases. Increase in maximum tensile and compressive axial force of the beams and the change in beams rotation is also shown in this study.

Keywords: Progressive collapse, Finite Element (FE), High strain rate, Reinforced Concrete (RC), Sub-assembly

ORIGINAL ARTICLE
 PII: S225204301500035-5
 Received 23 May, 2015
 Accepted 20 Sep, 2015

INTRODUCTION

Progressive collapse is a field of research which has become popular in recent years. Natural catastrophes such as 1994 Northridge earthquake, 1995 Kobe earthquake, and manmade disasters such as 1995 bombing of Murrah Federal Building and 2001 terrorist attack to the World Trade Center caused the failure of structural elements and progressive collapse of the building (ASCE, 2006). Research shows that in many of these catastrophes, progressive collapse is a dynamic event with high strain rate, when strain rate plays an important role in collapse pattern and response of building to the load. The first analytical research done in the field of progressive collapse of frames was carried out by Casciati et al. (1984). Progressive failure reliability of seismic analysis of 2D RC frames was considered in their research. Some researchers used simple modelling techniques to simulate the progressive collapse instead of using complex nonlinear dynamic analysis. Grierson et al. (2005), Izzuddin et al. (2008), Powell (2005), Vlassis (2007) and Ruth et al. (2006) utilized nonlinear static analysis with some provisions to consider the dynamic effects in a loading process. In addition, some nonlinear static analysis for progressive collapse were outlined in DoD (2005) and GSA (2003) guidelines. In order to consider the effects of dynamic loads, dynamic amplification factor (DAF) was used in loading process in research done by Ruth et al. (2006) and Grierson et al. (2005). Researchers such as Powell (2005), Dusenberry et al. (2004), Izzuddin et al. (2008), Vlassis (2007) used a process based on equilibrium of internal and external energies to analyze progressive collapse. Vlassis (2007), Izzuddin et al.

(2008), and Dusenberry et al. (2004) used a nonlinear static analysis (pushover) which considers the dynamic effects of abrupt removal of column. The static pushover analysis was according to a criterion that estimates deformation at the instant when kinetic energy was zero during progressive collapse. Marjanishvily et al. (2006) showed that the dynamic effects of column removal could not be overlooked. Using the process described in GSA guideline Kwasniewski (2010) applied blast loads to an existing 8-story steel frame building for analysing progressive collapse. However blast load is a dynamic load with high strain rate, Kwasniewski did not discuss the role of strain rate in his analysis. The same analysis for a RC building was done by Luccioni et al. (2004). Hao et al. (2006) and Shi et al. (2007, 2008, 2010) also used blast loads without considering the effects of strain rate in progressive collapse analysis of buildings. Tavakoli et al. (2013 a, and b) studied the dynamic response of 2D steel moment frames in a column removal scenario. Strain rate effects were considered in their dynamic analysis which was created by the blast load (Tavakoli et al., 2013b). Their research was done for steel structures and the dynamic effects of strain rate on concrete structures were not mentioned. Review of the past studies on progressive collapse shows that most of the research was done in static mode. In this research, the real behavior of sub-assembly in a progressive collapse scenario was considered with utilizing the effects of strain rate applied to materials. First, load transmission mechanism of sub-assemblages subjected to progressive collapse was discussed.

Furthermore, using the existing theories that specified the strain rate sensitivity of the material, FE

model of two sub-assemblages (Jan et al., 2011) was prepared in ABAQUS 6.13. The accuracy of the modeling was verified by comparing the FE results with experimental results in the static mode (Jan et al., 2011). Finally, by keeping constant the elements type, mesh, boundary conditions, interaction of concrete-steel, and with only increasing the loading rate, sub-assemblages behavior was predicted at high strain rate mode

Progressive Collapse

Progressive collapse is a chain reaction which initiates by loss of one or many load-bearing members. The initiator of progressive collapse may be man-made events such as explosion, fire and collision of vehicles. Progressive collapse can also be initiated by natural hazards such as earthquake. Removal of a structural element imposes additional loads to other structural members and causes the change in loading pattern (Nair, 2006). The mechanism of load transmission in a sub-assemblage subjected to removal of middle column is classified in three steps: arch action, formation of plastic hinges and catenary action (Nist, 2010).

Arch action: The compressive force creates in the upper side of the beams, near middle connection and in the lower side close to outer columns. The lower parts of the beams adjacent to middle connection and upper side of beams close to the outer connections become fractured because of tensile stresses (Nist, 2010).

Formation of plastic Hinges in Beams: Bars start to yield near fractured zones. The concrete in compressive zone sustains higher stresses, which causes crushing of

concrete. After the formation of plastic hinge, arch action still exists, but vanishes by increasing the middle joint displacement. The compressive force in beams, decreases in this stage and returns to its initial condition (Nist, 2010).

Catenary Action in beams: With increasing the middle joint displacement, concrete fractures throughout the whole specimen. The bars that were initially under compression start to sustain tension. Therefore, all of the applied loads are transferred to the bars and the role of concrete capacity is overlooked (Nist, 2010).

MATERIAL AND METHODS

Description of specimens

Each of the sub-assemblages have two beams and three columns in which the middle column is removed. Specimens were designed in scale of 1/2 according to the ACI 318-05 code. One of the specimens was designed at high ductility (seismic design) with dense stirrups. The other was designed in intermediate ductility (non-seismic design) (Jan et al., 2011). Geometry, dimensions and diameter of the specimens are shown in Figure 1 and Table 1. All given numbers are in millimetres. More details could be found in (Jan et al., 2011).

Table 1. Diameter of bars

Steel	T6	T10	T13
Diameter (mm)	6	10	13

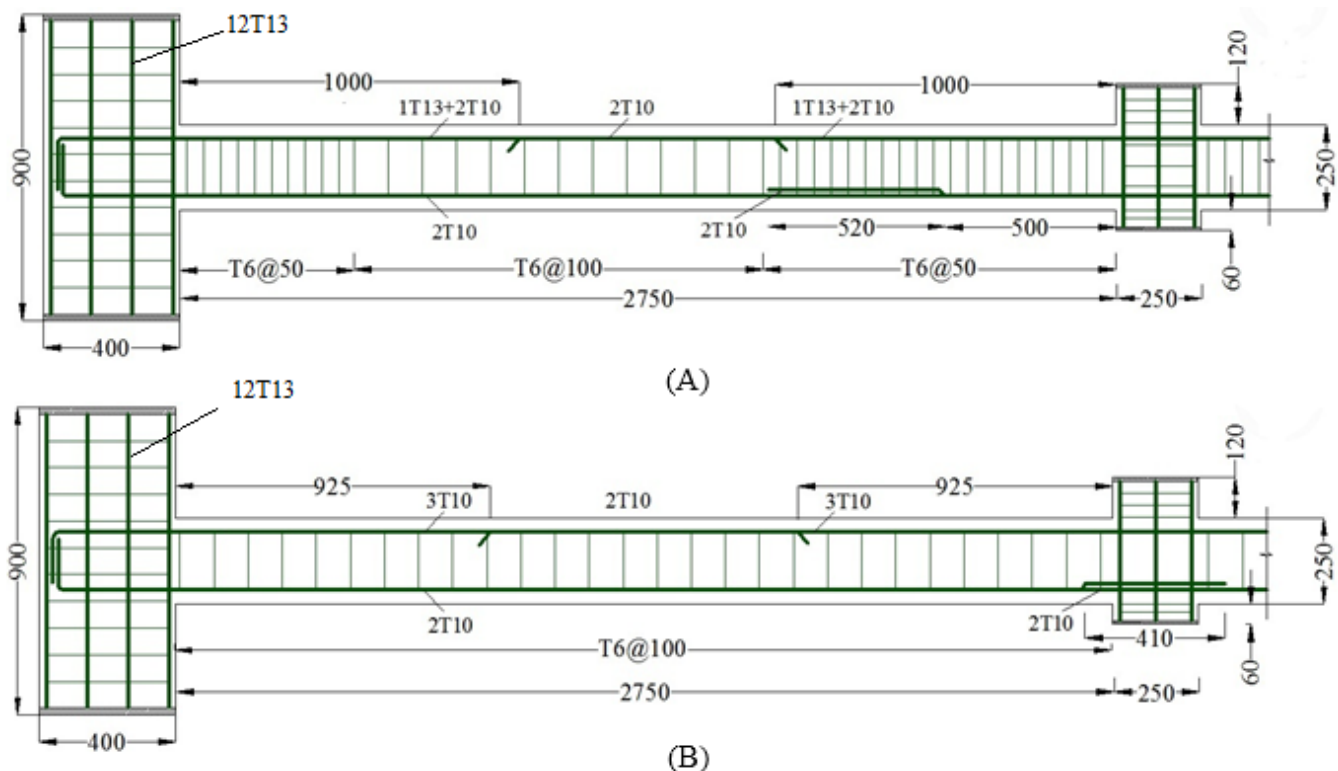


Figure 1. Geometry of specimens; A. Seismic design (S1); B. Non-seismic design (S2).

Behaviour at high strain rate

FE modelling of materials under static and dynamic loading requires knowledge of materials' sensitivity to the strain rate. Existing theories (Malver, 1998a,b; FIB, 2008)

were used to consider the sensitivity of materials to the strain rate. Experimental data for similar sub-assemblages subjected to explosion, shown that the strain rate in materials changed in the range of 0.01 to 0.1 1/s (Jan et

al., 2014). In order to simulate this condition in FE model in a conservative mode, the changes of steel and concrete strength under static strain rate of 0.001 s^{-1} up until dynamic strain rate of 1 s^{-1} were applied. ABAQUS calculated the strength of steel and concrete in different parts of the specimens according to the strain rates created in the materials during the loading time (ABAQUS, 2013).

Concrete in Compression with Different Strain Rates: International Federation for Structural Concrete (FIB) has investigated the dependence of compression in concrete with different strain rates (FIB, 2008). Some studies were carried out by Malver and Crawford (FIB, 2008) to consider the effects of strain rate on concrete module of elasticity and dynamic increase factor (DIF). DIF is the ratio of dynamic to static strength. Equations 1 and 2 were given for compression in concrete under the effects of strain rate (FIB, 2008; Malver, 1998a).

In which E_c = module of elasticity at strain rate $\dot{\epsilon}$, $E_{c,st}$ = static modulus of elasticity, f_c = compressive strength of concrete at strain rate $\dot{\epsilon}$, $f_{c,st}$ = static strain rate equal to $3 \times 10^{-5} \text{ s}^{-1}$, $\log(\gamma_s) = 6.156\alpha_s - 2$ and $\alpha_s = 1/(5+9f_{c,st}/10)$.

$$\frac{E_c}{E_{c,st}} = \left(\frac{\dot{\epsilon}}{\dot{\epsilon}_{st}}\right)^{0.026} \quad 1)$$

$$DIF_{conc}^{comp} = \frac{f_c}{f_{c,st}} = \begin{cases} \left(\frac{\dot{\epsilon}}{\dot{\epsilon}_{st}}\right)^{1.026\alpha_s} & \text{for } \dot{\epsilon} \leq 30 \text{ s}^{-1} \\ \gamma_s \left(\frac{\dot{\epsilon}}{\dot{\epsilon}_{st}}\right)^{1/3} & \text{for } \dot{\epsilon} > 30 \text{ s}^{-1} \end{cases} \quad 2)$$

Concrete in Tension with Different Strain Rates: Concrete under tension is also affected by strain rate. Equations 3 and 4 are given for concrete under tension with the influence of strain rate (FIB, 2008; Malver, 1998a).

$$\frac{E_c}{E_{c,st}} = \left(\frac{\dot{\epsilon}}{\dot{\epsilon}_{st}}\right)^{0.026} \quad 3)$$

$$DIF_{conc}^{tens} = \frac{f_t}{f_{t,st}} = \begin{cases} \left(\frac{\dot{\epsilon}}{\dot{\epsilon}_{st}}\right)^{1.016\delta_s} & \text{for } \dot{\epsilon} \leq 30 \text{ s}^{-1} \\ \beta_s \left(\frac{\dot{\epsilon}}{\dot{\epsilon}_{st}}\right)^{1/3} & \text{for } \dot{\epsilon} > 30 \text{ s}^{-1} \end{cases} \quad 4)$$

In which E_c = modulus of elasticity at strain rate $\dot{\epsilon}$, $E_{c,st}$ = static modulus of elasticity, f_t = tensile strength of concrete at strain rate $\dot{\epsilon}$, $f_{t,st}$ = static tensile strength of concrete, $\dot{\epsilon}$ = strain rate, $\dot{\epsilon}_{st}$ = static strain rate equal to $3 \times 10^{-6} \text{ s}^{-1}$, $\log(\beta_s) = 7.11\delta_s - 2.33$, $\delta_s = 1/(5+6f_{c,st}/10^7)$.

Steel with Different Strain Rates: Steel modulus of elasticity is independent of strain rate and is constant during loading. However, yield and ultimate strengths of steel are strain rate dependent. With increasing strain rate, the yield (F_y) and the ultimate (F_u) strengths of steel increase and the ultimate strain decreases (Malver, 1998b).

Malver proposed relations for effects of strain rate on steel, which are given in equations 5 and 6 (Malver, 1998b). The relations are similar in tension and compression.

$$DIF_{steel}^y = \frac{f_y}{f_{y,st}} = \left(\frac{\dot{\epsilon}}{\dot{\epsilon}_{st}}\right)^{\alpha_y} \quad 5)$$

$$DIF_{steel}^u = \frac{f_u}{f_{u,st}} = \left(\frac{\dot{\epsilon}}{\dot{\epsilon}_{st}}\right)^{\alpha_u} \quad 6)$$

In which f_y = yield strength of steel at strain rate $\dot{\epsilon}$, $f_{y,st}$ = static yield strength of steel, f_u = ultimate strength at strain rate $\dot{\epsilon}$, $f_{u,st}$ = static ultimate strength of steel, $\dot{\epsilon}$ = strain rate, $\dot{\epsilon}_{st}$ = static strain rate equal to 10^{-4} s^{-1} , $\alpha_y = 0.074 - 0.040 f_y / 414$, and $\alpha_u = 0.019 - 0.009 f_y / 414$.

With considering equations 1 to 6, material sensitivity to the strain rate was obtained. Table 2 to 5 shows the properties of concrete and steel in static and high strain rate mode, with strain rate range of 0.001 1/s to 10 1/s. During the analysis, ABAQUS calculates the amount of strain, strength and elasticity modulus using interpolation of entered data (Shi et al., 2011; ABAQUS, 2013).

Table 2. Material properties of bar T10

Strain rate (1/s)	Yield strength (MPa)	Ultimate strength (MPa)	Modulus of elasticity (MPa)
static	511	622	211.02
0.001	540	633	211.02
0.01	572	644	211.02
0.05	595	652	211.02
0.1	606	656	211.02
1	641	668	211.02
10	678	680	211.02

Table 3. Material properties of bar T13

Strain rate (1/s)	Yield strength (MPa)	Ultimate strength (MPa)	Modulus of elasticity (MPa)
static	494	593	185.873
0.001	524	604	185.873
0.01	557	615	185.873
0.05	581	624	185.873
0.1	592	627	185.873
1	629	639	185.873
10	668	652	185.873

Table 4. Material properties of bar T6

Strain rate (1/s)	Yield strength (MPa)	Ultimate strength (MPa)	Modulus of elasticity (MPa)
static	310	410	199.177
0.001	343	421	199.177
0.01	380	433	199.177
0.05	407	441	199.177
0.1	420	445	199.177
1	465	457	199.177
10	514	470	199.177

Table 5. Material properties of concrete

Strain rate (1/s)	Compressive strength (Mpa)	Tensile strength (Mpa)	Modulus of elasticity (Mpa)
static	32	3.2	663.27
0.001	35.59	3.91	726.581
0.01	38.16	4.24	771.409
0.05	39.8	4.28	804.437
0.1	40.93	5.59	819.002
1	43.89	4.97	869.531
10	47.07	5.39	923.177

FE Modelling:

Modeling Concrete Behavior: Concrete Damage Plasticity was used for modeling concrete behavior in this research. This model was introduced by Lubliner et al. (1989) and was completed with other researcher (By et al., 1998). The model can consider the sensitivity of materials to the strain rate. William-Warnke criterion was used for concrete failure in this study (Tomasz et al., 2005) (ABAQUS, 2013).

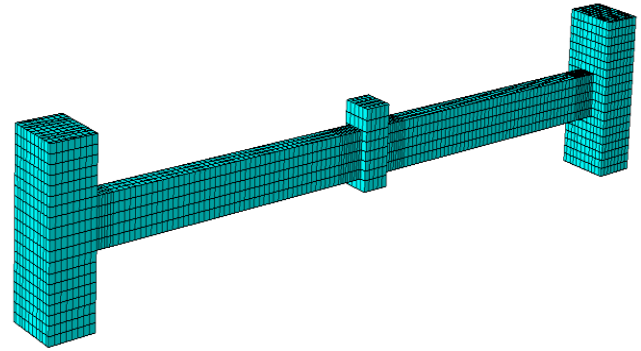
Modeling Steel Behavior: Bars were modelled separately with real dimensions. An Elasto-Plastic constitutive theory was used for modelling steel (Lykidis et al., 2008) (Satadru et al., 2012). Von mises yielding criterion was used to show the failure of steel (ABAQUS, 2013).

Concrete and Steel Interaction: The interaction between concrete and steel is an important parameter in RC structures. Embedded Element technique was used for modelling the interaction between concrete and steel. This simulation technique is useful in static and dynamic analyses (Lykidis G.C et al., 2008) (Satadru D et al., 2012; ABAQUS, 2013). The slippage between concrete and steel was overlooked in this study.

Choosing Elements: C3D8R element was used for FE modelling of concrete elements in ABAQUS. This is a 3D solid element with eight nodes and reduced integration method is used for solving integrals. Bars were modelled with T3D2 element which is a regular linear truss element with two nodes (ABAQUS, 2013).

Mesh: Mesh size for specimens was obtained using the proposed method in (Tavakoli et al, 2013b). 50 mm and 70 mm mesh size were used for solid and truss elements respectively. For regions of beam connections in

which experience critical conditions, finer mesh of 30 mm was utilized. Figure 2 shows mesh details of specimens.

**Figure 2.** Mesh detail**RESULTS AND DISCUSSION****Validation of modelling with static results:**

Displacement control loading with the rate of 0.1 mm/s was applied to the middle connection until failure of the specimens occurred. The criterion for final collapse was fracture of upper bars at connection of beams to the outer columns (Jan et al., 2011). Experimental results in static mode of two specimens were used to validate FE modelling (Jan et al., 2011). Figure 3 shows the ultimate deformation of specimens after failure.

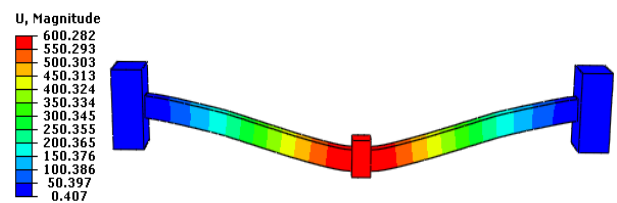
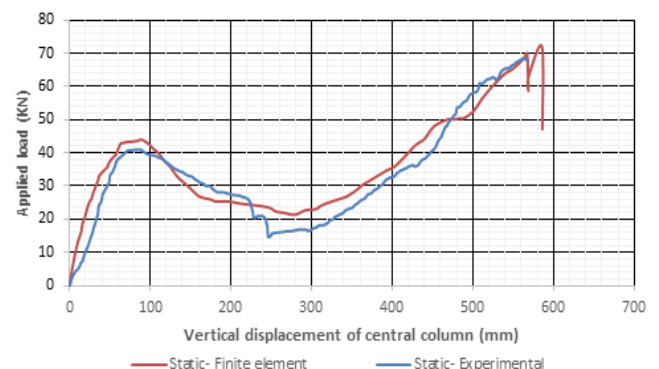
**Figure 3.** Displacement contours after failure

Figure 4 and 5 show applied load versus vertical displacement of middle column for S1 and S2 specimens. FE results showed good agreement with experimental results in static mode. There is a slight difference in experimental and FE results, which is due to homogeneity of materials and continuous interaction between concrete and steel in FE model. These cases do not occur in the experimental conditions because of experiment errors and loss of experiment accuracy.

**Figure 4.** Applied load versus vertical displacement of central column under static loading (specimen S1)

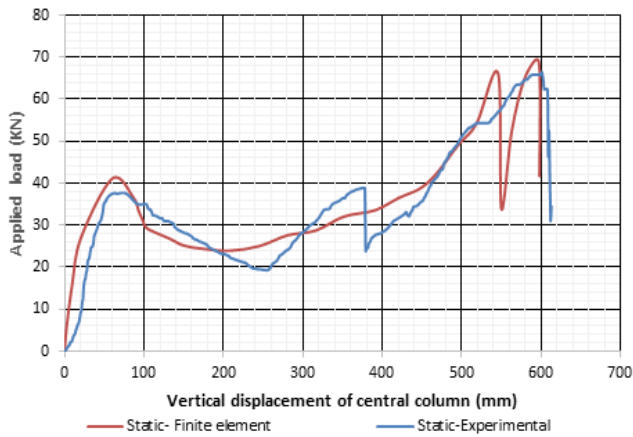


Figure 5. Applied load versus vertical displacement of central column under static loading (specimen S2)

Analysis at high strain rate:

After validation of modelling, using the same geometry, bar percentage, materials, boundary conditions, element type, mesh size, and just by increasing the loading rate at middle connection the analysis of specimens was done at high strain rate. Explosion experiment on the corresponding frames indicated that after removal of column, the middle connection moved downward at the speed of approximately 1000 mm/s due to the dead load (Jan et al., 2014). Figure 6 shows the vertical displacement history of middle connection after explosion. Therefore, load rate of 1000 mm/s was utilized for FE analysis of specimens in high strain rate mode in this study.

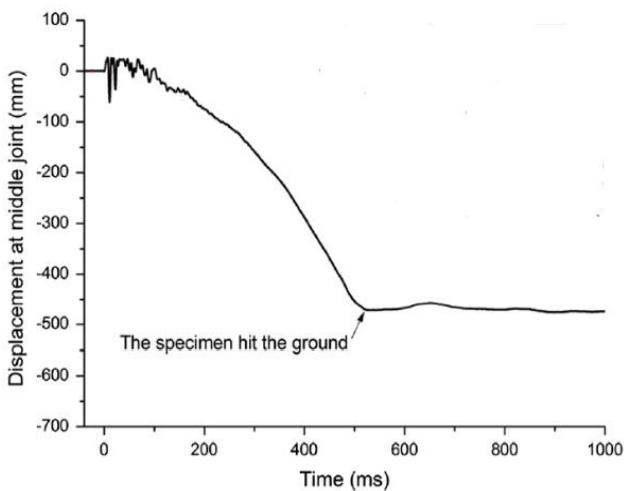


Figure 6. Displacement history of middle connection in blast experiment (Jan Y et al., 2014)

Strength of Specimens:

Specimen S1: Figure 7 shows applied load versus vertical displacement of central column at high rate loading for specimen S1. Due to the lack of experimental data at high strain rate for sub-assemblages, FE dynamic results were compared with the validated FE static results. Results showed that the maximum strength at the beginning of arch action increased 52% compared to the static mode. The ultimate displacement of middle

connection and the ultimate strength capacity of specimen reduced at high strain rate compared to the static mode. This can be partly attributed to the addition of inertia force due to the fast dynamic loading. The inertia effect does not contribute in static loading, because the rate of loading is low and the time of loading is long. Sudden drops in curve show fracture of bars due to increased stress at the critical points during loading. Applied load curve shows that the failure mode of bars has changed at high rate loading compared to the static case. First fracture occurred in lower bars at connection of beam to middle column, and the load bearing capacity decreased accordingly. Figure 8 shows Maximum Principle stresses of middle connection bars in specimen S1 before and after fracture at high strain rate. After the lower bars at the connection of beam to middle column were broken, upper continuous bars of the beams started to carry applied load. With further increasing the vertical displacement of the middle connection, the stress in upper bars of the beams at the right connection reached to the critical value then broke. Figure 9 shows the ultimate displacement and fracture of bars for specimen S1.

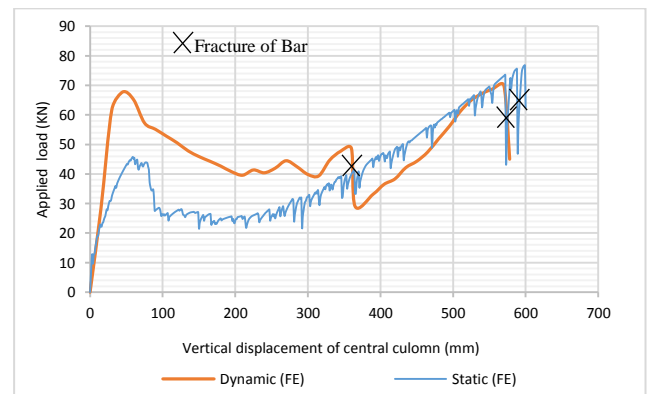


Figure 7. Applied load versus vertical displacement of middle column at high strain rate loading (specimen S1)

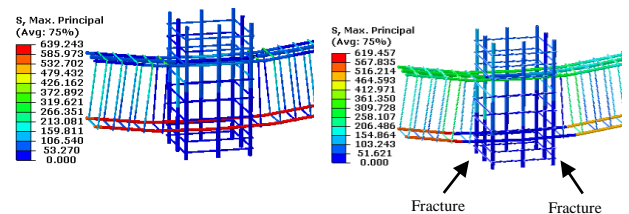


Figure 8. Middle connection of S1 specimen; A. Before fracture of bars; B. After fracture of bars

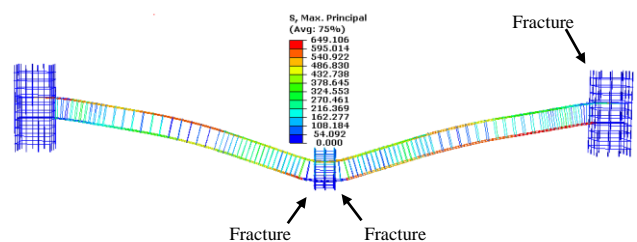


Figure 9. Ultimate failure of specimen S1 and fracture of bars

Specimen S2: Applied load versus vertical displacement of middle column at high strain rate for specimen S2 is displayed in Figure 10. This curve shows that the maximum load at the beginning of the arch action increased 44% compared to the static case. Similar to the specimen S1, the ultimate displacement and the ultimate strength capacity of specimen S2 decreased due to the inertia force effect. The lower bars of the beams in specimen S2 were spliced near middle connection. Hence, this zone encountered high stress concentration. The first bar fracture occurred in the left side of middle connection at the splice zone.

Figure 11 shows Maximum Principle stresses in bars at middle connection before and after fracture of left side bars. After that, right side bars of middle connection broke. With increasing the vertical displacement of middle connection, beam upper bars at the left side connection broke and beam reached the final collapse. Figure 12 shows ultimate displacement and failure of bars in specimen S2.

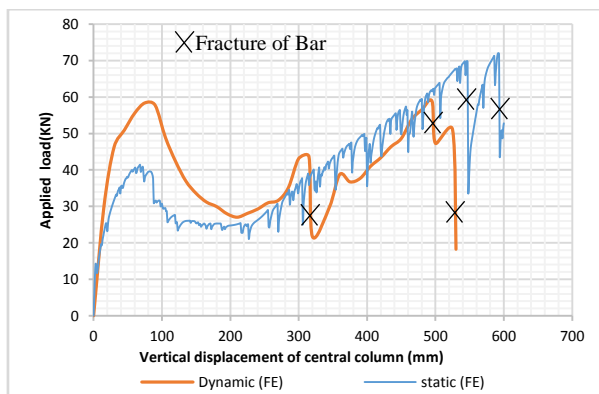


Figure 10. Applied load versus vertical displacement of middle column at high strain rate loading (specimen s2)

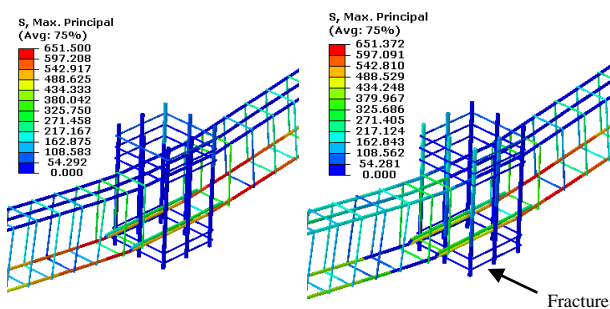


Figure 11. Middle connection of S2 specimen; A. Before fracture of bars; B. After fracture of bars

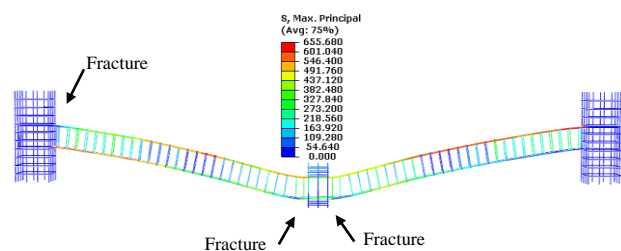


Figure 12. Ultimate failure of specimen S2 and fracture of bars

The arch action of concrete for specimen S1 at high strain rate is shown in Figure 13. Because of similarity,

behaviour of specimen s2 is not discussed. With initiation of loading, concrete fractured in tension zones and compression zones remained intact in the form of an arch, Figure 13.A. With increasing the vertical displacement of middle connection, the arch action of concrete was terminated and the entire specimen was subjected to tension, Figure 13.B.

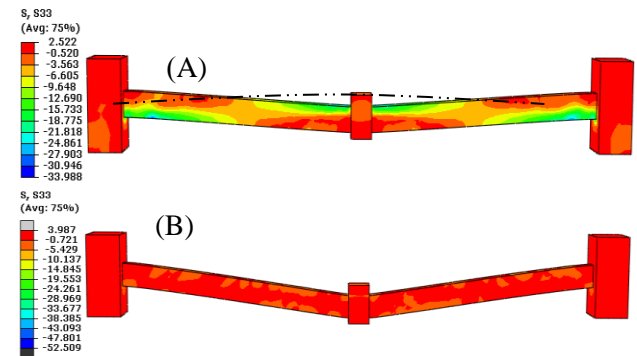


Figure 13. Resistance mechanism in concrete; A. Formation of arch action; B. Failure of concrete

Axial Force in Beams:

Axial force develops in beams due to the boundary condition of outer columns. These boundary conditions simulate side frames in actual buildings. Figures 14 and 15 show beam axial force versus vertical displacement of middle column for specimens S1 and S2. Positive and negative values of beam axial force display compressive and tensile force, respectively. Similar to the applied load curve, curves in Figures 14 and 15 show some abrupt drops in strength, which are due to the fracture of bars. Results show that the maximum compressive force increased 13% and 14% in specimen S1 and S2, respectively compared to the static case. Maximum tensile force of beams increased 20% and 26% in specimen S1 and S2, respectively compared to static mode. The range of compressive arch action at high strain rate was the same as static case. The range of tension in specimens decreased at high strain rate because of lower strength capacity. Experimental results of explosion load have shown that compressive range increased at high rate loading, however this phenomenon did not occur in FE analysis.

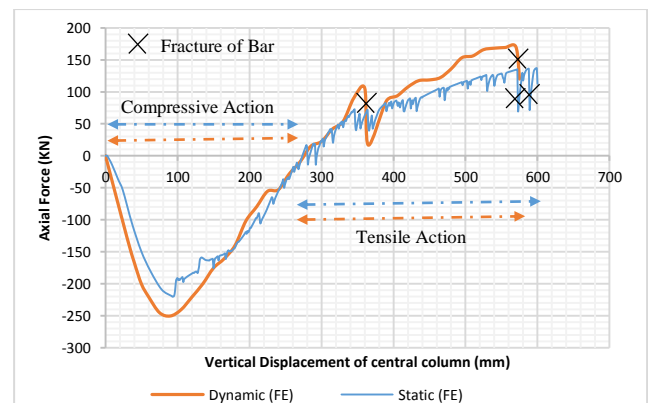


Figure 14. Axial force in beams for specimen S1

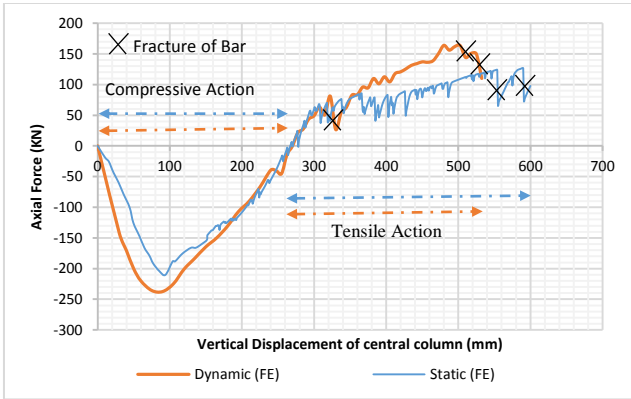


Figure 15. Axial force in beams for specimen S2

Rotation and Curvature of Beams:

Figure 16 shows the rotation in connections at the end of loading. The rotation of two beams in experimental conditions may not be the same due to experiment errors and non-homogeneity of materials. Because geometry and boundary condition are symmetric and the materials are homogeneous in FE model, the rotation of the two beams is approximately equal.

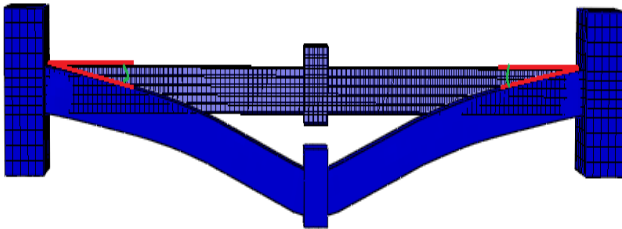


Figure 16. Rotation in beams

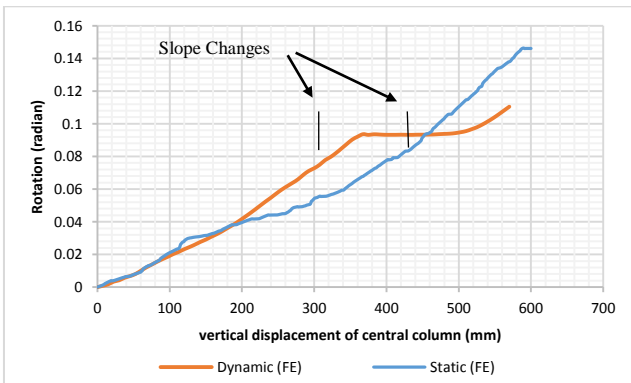


Figure 17. Rotation of beam at outer connections for specimen S1

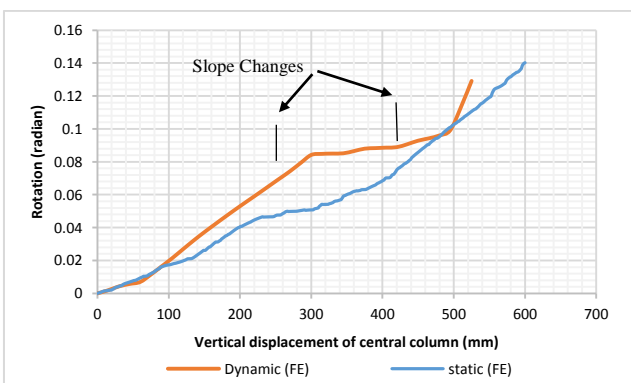


Figure 18. Rotation of beam at outer connections for specimen S2

Figure 17 and 18 show the rotation of beams versus vertical displacement of middle column for specimens S1 and S2 at high strain rate. According to these figures, the rotation of beams in both static and dynamic case has three steps with three different slopes.

At high strain rate, rotation increased linearly, and then it became constant. At the end, the rotation increased again until the specimen failure occurred. The changes of rotation in static case were not sensible because of long time and low rate of loading. Hence, the specimens had enough time for milder changes in rotation. As it can be seen from the Figures 17 and 18, the rotation increased with almost linearly slope in static mode. The ultimate rotation at the end of analysis in the static mode was more than the high strain rate case due to the less strength capacity of specimens at high strain rate.

CONCLUSION

Review of literature showed the importance of investigating the behaviour of sub-assemblages under high strain rate. Hence, this study considered the sensitivity of materials to strain rates with existing theories and incorporated them in FE model. The analysis results of sub-assemblages with high strain rate loading were compared with static analysis. FE Results showed that the strength of specimens in arch action zone increased and the vertical displacement of middle connection at the point of ultimate failure decreased at high strain rate compared to static mode. Failure pattern for bars at high strain rate was different to the static case. Results of axial force in beams showed that the maximum compressive and tensile force increased at high strain rate. Although the range of compressive action was the same in both static and high strain rate, the range of tensile action decreased at high strain rate. The rotation of beams showed a non-uniform behaviour at high strain rate compared to the static cases. The changes in rotation slope at high strain rate were more than the static case due to the low time of loading.

Due to the lack of sufficient experimental data at high strain rate range and also the cost of testing, the proposed model in this study is appropriate to predict the structural behavior in progressive collapse with considering the effects of strain rate.

REFERENCES

- ABAQUS Version 6.13 Documentation, (2013).
- An experimental and computational study of reinforced concrete assemblies under a column removal scenario (NIST, 2010). US Department of Commerce, National Institute of Standards and Technology.
- By JL, Gregory L (1998). Plastic damage model for cyclic loading of concrete structures, *J. Eng. Mech*, 124: 892-900.

- Casciati F, Faravelli L (1984). Progressive failure for seismic reliability analysis. *Engineering Structures*, 6(2): 97-103.
- Dusenberry D, Cagley J, Aquino W (2004). Case studies. Multihazard Mitigation Council national workshop on Best practices guidelines for the mitigation of progressive collapse of buildings. National Institute of Building Sciences (NIBS). Washington, D.C.
- Grierson DE, Xu L, Liu Y (2005). Progressive-failure analysis of buildings subjected to abnormal loading. *Computer Aided Civil and Infrastructure Engineering*, 20(3): 155-171.
- GSA (2003). Progressive collapse analysis and design guidelines for new federal office buildings and major modernization projects, The U.S. General Services Administration.
- Hao H, Wu C, Li Z, Abdullah AK. (2006). Numerical analysis of structural progressive collapse to blast loads. *Trans Tianjin Univ*, 12: 31-4.
- International Federation for Structural Concrete (FIB, 2008), Constitutive modelling of high strength/high performance concrete. State-of-art report. FIB Bulletin 42.
- Izzuddin BA, Vlassis AG, Elghazouli AY, Nethercot DA (2008). Progressive collapse of multi-story buildings due to sudden column loss - Part I: Simplified assessment framework. *Engineering Structures*, 30: 1308-1318.
- Jan Y, Kang HT (2011). Experimental and numerical investigation on progressive collapse resistance of reinforced concrete beam column sub-assemblages, *Journal of Engineering Structures*, Elsevier, Vol. 55, 90-106.
- Jan Y, Tassilo R, Alexander S (2014). Dynamic Progressive Collapse of an RC Assemblage Induced by Contact Detonation", *Journal of Structural Engineering*, ASCE, 140(6): 04014014.
- Kwasniewski L (2010). Nonlinear dynamic simulations of progressive collapse for a multistory building. *Engineering Structures*, 32: 1223-1235.
- Lubliner J, Oliver J, Oller S, Onate E (1989). A plastic-damage model for concrete. *International journal of Solids and Structure*, 25(3): 299-326.
- Luccioni BM, Ambrosini RD, Danesi RF (2004). Analysis of building collapse under blast loads. *Engineering Structures*, 26: 63-71.
- Lykidis GC, Spiliopoulos KV (2008). 3D Solid Finite Element Analysis of Cyclically Loaded RC Structures Allowing Embedded Reinforcement Slippage, *Journal of Structural Engineering*, 134(4): 629-638.
- Malver LJ, Crawford JE (1998a). Dynamic increase factors for concrete. 28th DDESB seminar, Orlando, FL, USA.
- Malver LJ, Crawford JE (1998b). Dynamic increase factors for steel reinforcing bars, 28th DDESB seminar, Orlando, FL, USA.
- Marjanishvili S, Agnew E (2006). Comparison of various procedures for progressive collapse analysis. *ASCE Journal of Performance of Constructed Facilities*, 20(4): 365-374.
- Minimum Design Loads for Buildings and Other Structures (2006). Structural Engineering Institute. ASCE Publications, 7: 5.
- NIST, Nair RS (2006). Preventing Disproportionate Collapse. *Journal of Performance of Constructed Facilities*, ASCE, 20(4): 309-314.
- Powell G (2005). Progressive Collapse: Case studies Using Nonlinear Analysis. *Structures Congress*, 1-14.
- Ruth P, Marchand KA, Williamson EB (2006). Static equivalency in progressive collapse alternate path analysis: reducing conservatism while retaining structural integrity, *Journal of Performance of Constructed Facilities*, 20(4): 349-364.
- Satadru D, Adhikary B.L, Kazunori, F. (2012). Dynamic behavior of reinforced concrete beams under varying rates of concentrated loading, *International Journal of Impact Engineering*, 47: 24-38.
- Shi Y, Li Z, Hao H (2007). Numerical analysis of progressive collapse of reinforced concrete frame under blast loading. *J PLA Univ Sci Technol (Natural Science Edition)*, 8(6): 652-658.
- Shi Y, Hao H, Li Z (2008). Numerical derivation of pressure impulse diagrams for prediction of RC column damage to blast loads. *International journal of Impact Engineering*, 35(11): 1213_27.
- Shi Y, Li Z.-X, Hao H. (2010). A new method for progressive collapse analysis of RC frames under blast loading. *Engineering Structures*, 32: 1691-1703.
- Tavakoli HR, Kiakojoouri F (2013a). Numerical Study of Progressive Collapse in Framed Structures: A New Approach for Dynamic Column Removal. *International journal of engineering, Transactions A: Basics*, 26(7): 685-692.
- Tavakoli HR, Kiakojoouri F (2013b). Influence of Sudden Column Loss on Dynamic Response of Steel Moment Frames under Blast Loading" *international journal of engineering, Transactions B: Applications*, 26(2): 197-205.
- Tomasz J, Tomasz O (2005). Identification of parameters of concrete damage plasticity constitutive model", *Foundations of Civil and Environmental Engineering*.
- UFC-DoD, UFC (2005). Design of Buildings to Resist Progressive Collapse, the U.S. Department of Defense.
- Vlassis AG (2007). Progressive collapse assessment of tall buildings, Ph.D. thesis. Department of Civil and Environmental Engineering, Imperial College London.